RESEARCH ARTICLE

Macromolecular Materials and Engineering
Open Access
www.mame-journal.de

The Effect of a Low Degree of Fluorine Substitution on Cotton Fiber Properties

*Ofir Aharon Kuperman, Peterson de Andrade, Tanguy Terlier, Jacob Judas Kain Kirkensgaard, Robert A. Field, and Filipe Natalio**

Cellulose modification often employs chemical processes to tailor its properties and functionalities to fit the demands of a wide range of applications, maximizing its potential as a versatile and sustainable material. From both synthetic and environmental standpoints, one of the ultimate goals is to achieve significant modifications to enhance the end properties of the cellulose while minimizing the number of modified building blocks. The current study demonstrates that a synthetic glucose derivative, 6-deoxy-6-fluoro-glucose (6F-Glc), fed into the fertilized cotton ovules, resulted in the accumulation of fluorine inside the cotton fibers with no apparent alteration to their morphology or development. These fibers exhibited a degree of substitution of 0.006, which is 170 times lower than that reported for chemical methods for cellulose modification. However, the physical characterization of the modified fibers showed a surprisingly large impact of this low-level modification on the cellulose structure (e.g., hydrogen bonding network rearrangement) and a modest increase in the mechanical properties of the fibers. The obtained results exemplify the use of biological systems to introduce low quantities of new functionalities while maximizing the impact on fiber properties.

1. Introduction

Homogeneous and heterogeneous phase chemistry methods are widely employed to directly replace cellulose hydroxyl groups in anhydroglucose units (AGUs) with other functional groups (e.g., esters, methyl, silyl, etc.).[1] This allows for specific customization of properties such as solubility, mechanical strength, compatibility with other materials, and thermal stability.[1b,e,j,2] In certain cases, this transformation can be achieved via indirect routes, including the production of intermediate compounds.[1j,3] The degree of substitution (DS) values in cellulose range from 0 to 3,[1j,4] and depends on the implementation of specific phase chemistry, the experimental conditions, and the chemistry-specific functional groups that result in the efficient replacement of the -OH groups [1c,2b,5]. The achievement of a low DS value, in conjunction with significant modifications of cellulose properties, is an ideal synthetic pathway for generating truly sustainable cellulose-based materials.[1a]

Several studies related to traditional chemistry methods have reported low DS values that significantly impact cellulose properties. For example, DS values as low as 0.1 for cellulose esters derivatives,[6] 0.2 for carboxymethyl cellulose from bacterial cellulose (*Gluconacetobacter xylinus*),[2b] and 0.24 for the preparation of cellulose succinates[7] and for homogeneous modification of cellulose with succinic anhydride in ionic liquid.[8] As

O. A. Kuperman, F. Natalio
Department of Plant and Environmental Sciences
Weizmann Institute of Science
Rehovot 761001, Israel
E-mail: filipe.natalio@weizmann.ac.il

P. de Andrade, R. A. Field
Manchester Institute of Biotechnology and Department of Chemistry
University of Manchester
Manchester M1 7DN, UK

T. Terlier
SIMS laboratory
Shared Equipment Authority
Rice University
Houston, TX 77005, USA

J. J. K. Kirkensgaard
Department of Food Science
University of Copenhagen
Copenhagen 1958, Denmark

J. J. K. Kirkensgaard
Niels Bohr Institute
University of Copenhagen
Copenhagen 2100, Denmark

R. A. Field
Iceni Glycoscience Ltd
Norwich Research Park
Norwich NR4 7TJ, UK

The ORCID identification number(s) for the author(s) of this article can be found under https://doi.org/10.1002/mame.202300337

DOI: 10.1002/mame.202300337

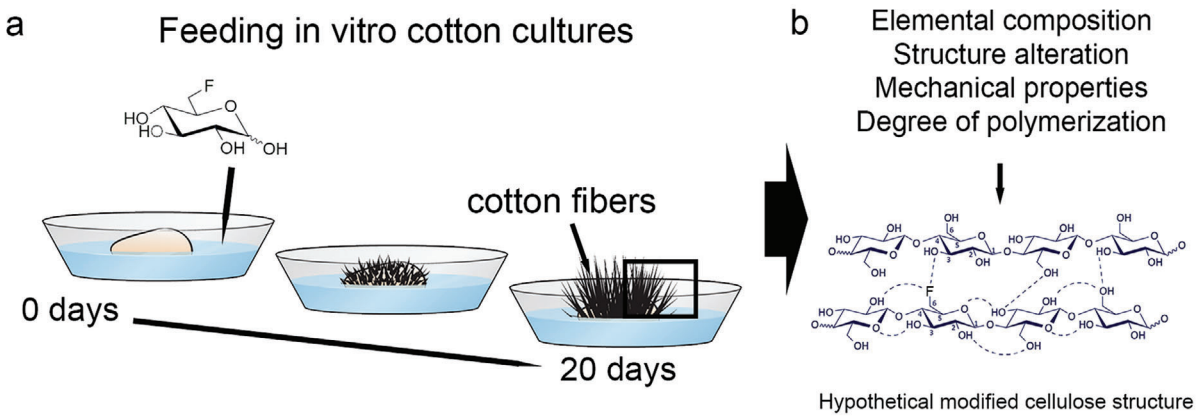

Figure 1. Schematic representation of the roadmap of this project illustrating the different steps, starting by a) feeding 6F-Glc to the growth medium floating cotton ovule in vitro cultures, b) fiber end properties assessment, and a proposed hypothetical structure on the incorporation of fluorine atoms into the cellulose structure.

for starch chemical modification, values of DS can get as low as 0.006 for octenyl succinic starch ester (OSA ester) by semi-dry method[9] or 0.06 for amaranth starch.[10]

Recently, several bio-based approaches have emerged as promising avenues for the modification of cellulose end properties. One approach involved in vitro enzymatic synthesis[11] of fluorinated celluloses[12] and their post-synthesis co- and self-assembly with nanocrystalline cellulose.[13] Another innovative method employed fertilized cotton ovules grown in vitro that were fed with different glucose derivatives.[14] Specifically, when 6-deoxy-6-fluoro-glucose-1-phosphate was fed to an in vitro cotton ovule system, it resulted in cotton fibers with a DS value of 0.06 (unpublished observations). Remarkably, the reported DS was 17 times smaller than that of the lowest obtained via traditional phase chemistry methods.[6] However, these fibers exhibited altered structural properties, including increased tensile strength and enhanced water retention.

2. Results and Discussion

In this study, we aimed to employ cotton ovule in vitro cultures to modify the cellulose fiber end properties by feeding glucose derivatives into the growth medium (**Figure 1**), providing a follow-up to our previous work[14] and expanding and redefining the limits of its applicability. Specifically, we investigated the impact of synthetic 6-deoxy-6-fluoro-glucose (6F-Glc) on ovule and fiber development in cotton (*Gossypium hirsutum* L.) in vitro cultures. We also explored the potential of this approach to enrich the cellulose fibers with fluorine atoms and its impact on the structural and mechanical properties of the resulting fibers (Figure 1).

2.1. Chemoenzymatic Synthesis Of 6-Deoxy-6-Fluoro-Glucose (6F-Glc) and Feeding to a Fertilized Cotton Ovule In Vitro Model

To support our studies, we developed a scalable chemoenzymatic synthesis of 6-deoxy-6-fluoro-glucose (6F-Glc). To achieve this, 6F-Glc was synthesized in a three-step process starting from commercially available α-D-glucose pentaacetate, achieving an overall yield of 56% (**Figure 2**), which is considered efficient for this type of synthesis. Briefly, the first step involved high-yielding regioselective deacetylation using *Candida rugosa* lipase[15] to afford the primary alcohol 1, thus facilitating selective access to the C6 position by avoiding extra protecting group steps. In steps 2 and 3, fluorination of the primary alcohol with diethylaminosulfur trifluoride (DAST)[16] gave 2 in reasonable yield, and final deprotection under Zemplén conditions[16] gave the corresponding fully deacetylated 6F-Glc (3) in near quantitative yield.

Then, we fed the synthetic 6F-Glc (5 µM) to fertilized *G. hirsutum* L. (cotton) ovule in vitro cultures collected 2 days post-anthesis (2 dpa). The presence of 6F-Glc did not confer any macroscopic impact on ovule and fiber development (**Figure 3**a,b), as found previously for the presence of 2-deoxy-2-iodo-D-glucose.[17] We measured and compared the fiber length, ovule length, ovule content, and fiber dry matter content between control ovules and those grown in the presence of 5 µM 6F-Glc (Figures 3d–g). Across all measurements, we found no statistically significant differences between the control and 6F-Glc fibers

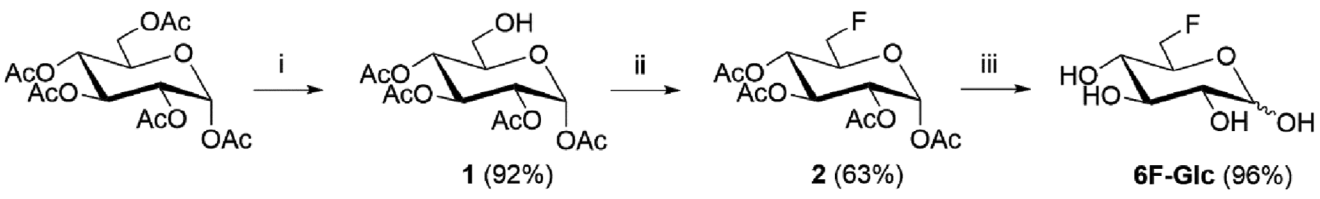

Figure 2. Chemoenzymatic route to the synthesis of 6-deoxy-6-fluoro-glucose (6F-Glc): i) Lipase, phosphate buffer pH 4, dioxane, 24 h at 30 °C; ii) DAST, collidine, DCM; iii) $NaOCH_3$, MeOH, Dowex H^+.

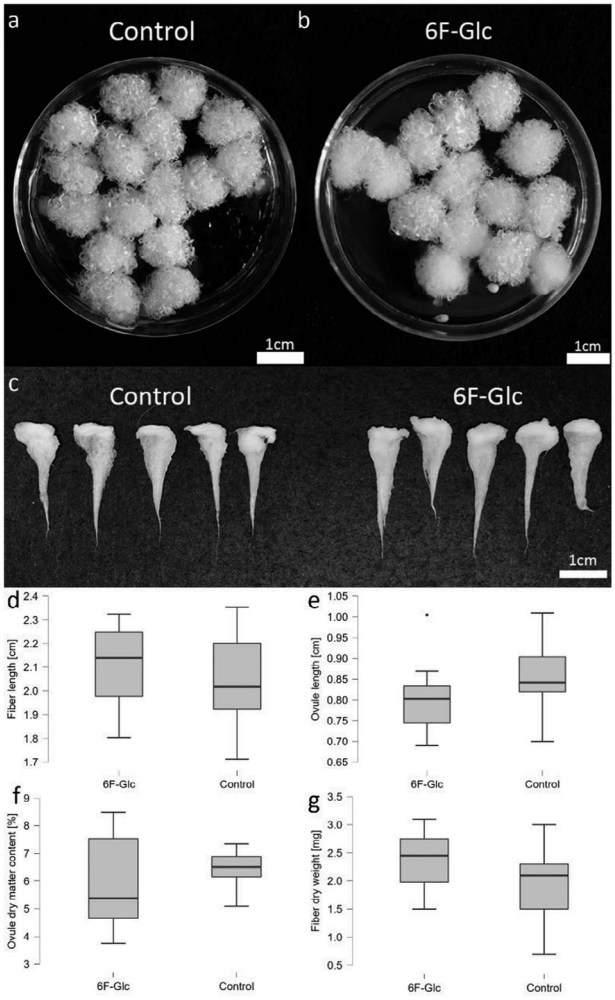

Figure 3. a) Representative photographic images of the fertilized cotton ovule in vitro cultures without any additive and b) incubated with 6-deoxy-6-fluoro-glucose (6F-Glc, 5 µM), showing that the presence of 6F-Glc does not have any macroscopic effect. c) Representative images of cotton ovules with the combed fibers after standard growth conditions in the absence (left set) or presence of 5 µM 6F-Glc (right set). c–f) Comparative box plots of the c) fiber length, d) ovule length, e) ovule dry weight content, and f) fiber dry weight of the cotton ovules after standard growth conditions in the absence or presence of 5 µM 6F-Glc. None of the measurements showed a statistically significant difference between the control and 6F-Glc ovules and fibers. Panels (d,e,g): $N = 10$, Brown–Forsythe, p-value > 0.05. t-test, p-value > 0.05. Panel (f): $N = 10$, Brown–Forsythe, p-value < 0.05. Welch, p-value > 0.05.

(panels (d,e,g): $N = 10$, Brown–Forsythe, p-value > 0.05; t-test, p-value > 0.05. For panel (f): $N = 10$, Brown–Forsythe, p-value < 0.05; Welch, p-value > 0.05).

We then focused on the physical characterization of the fibers. The fibers excised from cotton ovules fed with 5 µM 6F-Glc are referred to as "6F-Glc fibers," and those excised from the ovules grown in the absence of any additives as "control fibers". We started by using backscattered scanning electron microscopy (BSE-SEM) to assess any morphological and fiber width differences between control and 6F-Glc fibers. In both cases, the fibers displayed a flattened ribbon-like morphology (Figure S1, Supporting Information), which is typically attributed to immature fibers.[18] The average fiber width was not statistically different between 6F-Glc and control fibers ($N = 25$, t-test, p-value > 0.05), with values of 27.6 ± 3.2 and 28.1 ± 5.9 µm for 6F-Glc and control fibers, respectively.

2.2. Determination of Cellulose Degree of Substitution (DS) by Elemental Analysis

We started by measuring the presence of fluorine in the control and 6F-Glc fibers. We found 0.067 ± 0.02% w/t content of fluorine in the 6F-Glc fibers. This value was statistically significantly different than the control fibers ($N = 12$ for each treatment, p-value < 0.05). Additionally, the determined fluorine content equated to a DS of 0.006 ± 0.002, as calculated by Equation (1). Specifically, for every 1000 AGU units, six hydroxyl groups were substituted. DS at 0.006 is 170 times smaller than the lowest DS values reported in the existing literature on the chemical modification of cellulose, which range from 0.1 to 0.24.[2b,6–8] A DS value of 0.006 is similar to that found for the chemical esterification of starch by octenyl succinic ester (OSA ester) (DS = 0.006).[9]

This value is 17 times smaller than the lowest reported value achieved by the phase chemistry methods (DS 0.1)[6] However, the presence of fluorine could indicate either its incorporation into the material or surface contamination, especially given the low amounts.

2.3. Mapping 6F-Glc into Cotton Fibers by Time of Flight-Secondary Ions Mass Spectrometry (ToF-SIMS)

To rule out any suspicion of surface contamination, we performed ToF-SIMS depth profile analysis on both control and 6F-Glc fibers for F^- (m/z 18.99) and OH^- (m/z 17.00) ions (**Figures** 4a and b). For the F^- ion depth profile, we found its presence in higher concentrations in 6F-Glc fibers than in control fibers, followed by logarithmic decay in 6F-Glc fibers as a function of the depth, indicating that the presence of fluorine throughout the thickness of the fibers (Figure 4a) confirming the presence of fluorine inside the fibers, and indicative that the presence of fluorine was not caused by non-specific cellulose fiber surface contamination. In the case of the OH^- group depth profile (Figure 4b), we found a logarithmic increase profile for control fibers through all the collected data points. For the 6F-Glc fibers, we found a different profile, that is, there is a small logarithmic increase of the hydroxyl groups in the initial data points followed by a plateau. These results suggest an alteration of OH content throughout the fibers, reinforcing the notion that 6-deoxy-6-fluoroglucose is incorporated into cellulose fibers.

We compared the cellulose inter- and intra-chain hydrogen bonding network of 6F-Glc and control fibers using the -OH stretching modes located in the 3800–3000 cm^{-1} region of the Fourier-transform infrared (FT-IR) spectra.[19] We found that the OH^-stretching band is red-shifted in 6F-Glc fibers compared to control fibers, that is, it is centered at 3347 and 3376 cm^{-1} for 6F-Glc (**Figure** 5a) and control fibers, respectively (Figure S2a, Supporting Information). Peak fitting and deconvolution of the same

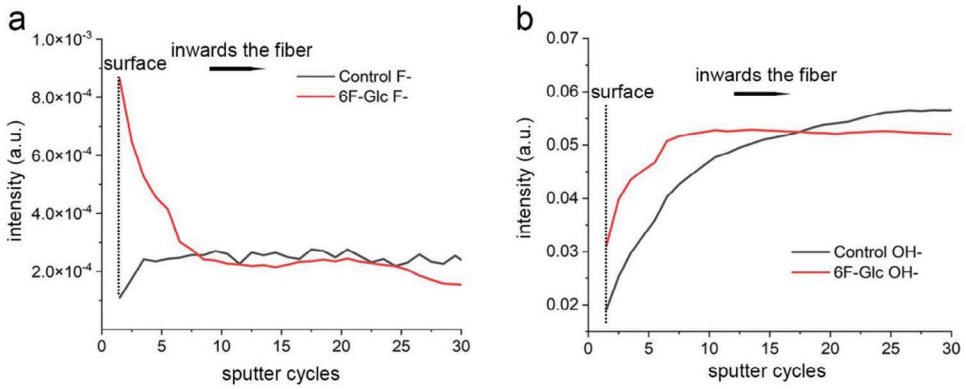

Figure 4. a,b) Depth profiles of the chemical distribution of a) F^- ions (m/z 18.99) and b) OH^- ions (m/z 17.00) from the surface inwards of the cotton fibers for the control fibers (black lines) and 6F-Glc fibers (red lines), indicating the presence of fluorine throughout the thickness of the whole fibers and an alteration of the OH quantities as a function of depth profile.

region for 6F-Glc fibers revealed the interchain H-bond band corresponding to O(6)H—O(3') (Figure 5a and Figure S2a, Supporting Information, red line) and the intrachain H-bond band corresponding to O(3)H—O(5) (Figure 4a and Figure S2a, Supporting Information, green line) was blue-shifted. More specifically, the interchain H-bond O(6)H—O(3') was shifted from 3545 to 3563 cm^{-1}, whereas that of O(3)H—O(5) was shifted from 3410 to 3430 cm^{-1}. In contrast, the band corresponding to the intrachain H-bond O(2)H—O(6) was red-shifted. Additionally, this band shifted from 3286 cm^{-1} in the control fibers to 3274 cm^{-1} in the 6F-Glc fibers (Figure 5a and Figure S2a, Supporting Information, dark blue line). The presence of small amounts of 6F inside the fibers resulted in an altered H-bond network, where the interchain O(6)H—O(3') and intrachain O(3)H—O(5) increased in strength upon modification, and O(2)H—O(6) decreased in strength.

The wide-angle X-ray scattering (WAXS) diffraction pattern of 6F-Glc fibers and the theoretical curves from the relevant cellulose polymorphs are shown in Figure 5b (red line). The naming convention and unit cell definitions were adopted from the literature.[20] The scattering patterns for the radially averaged intensity were recorded as a function of the magnitude of the scattering vector (Equation (2)). The presence of 6F-Glc inside the cotton fibers induced small recrystallization with no apparent reduction of the crystallinity compared to the control fibers (Figure S2b, Supporting Information). The 6F-Glc fibers are composed predominantly of a mixture of cellulose I_α and I_β polymorphs, similar to that of the control fibers. However, their ratio differs in favor of I_α for the 6F-Glc. Further, we also detected the presence of small contributions of cellulose $I_{III,I}$ -like structure, as indicated by a pronounced shoulder at $q \sim 1.5$ $Å^{-1}$ (Figure 5b) compared to the control fibers (Figure S2b, Supporting Information). However, the low DS value did not immediately suggest the presence of the cellulose $I_{III,I}$ allomorph. Thus, based on the current data, we could not unambiguously assign this modification to the allomorph cellulose $I_{III,I}$.

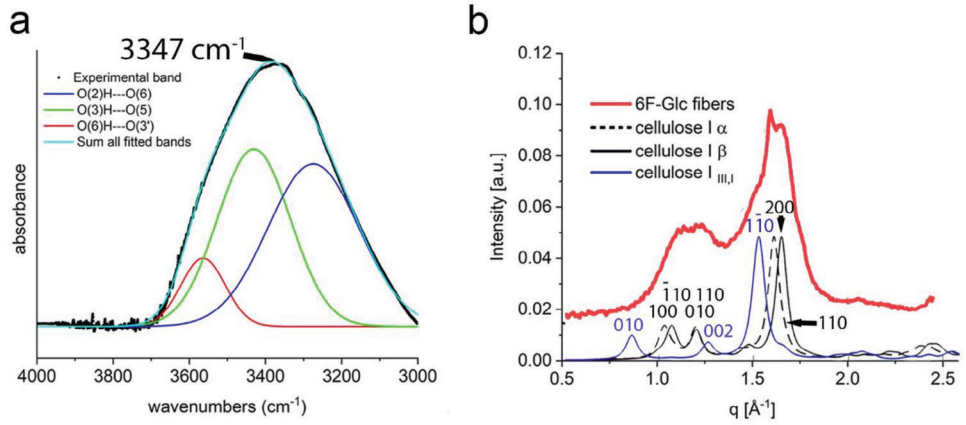

Figure 5. a) Representative deconvoluted normalized FT-IR spectra of 6F-Glc fibers showing the peaks attributed to intramolecular H-bonds O(3)H—O(5) (green line) and (2)H—O(6) (blue line) and one intermolecular bond O(6)H—O(3') (red lines). 6F-Glc shows the weakening of the intermolecular hydrogen bonds and the strengthening of the intramolecular hydrogen bonds compared to the control fibers. b) WAXS diffraction data from 6F-Glc (red line) shows that they are composed predominantly of a mixture of cellulose I_α and I_β with an increase of I_α and a smaller contribution of cellulose $I_{III,I}$-like allomorph and slight recrystallization compared to the control fibers. Simulated diffraction curves based on crystallographic data for cellulose polymorphs are shown under the experimental WAXS diffraction curves: black dashed line): cellulose Iα; black solid line: cellulose Iβ; and blue line: cellulose $I_{III,I}$.

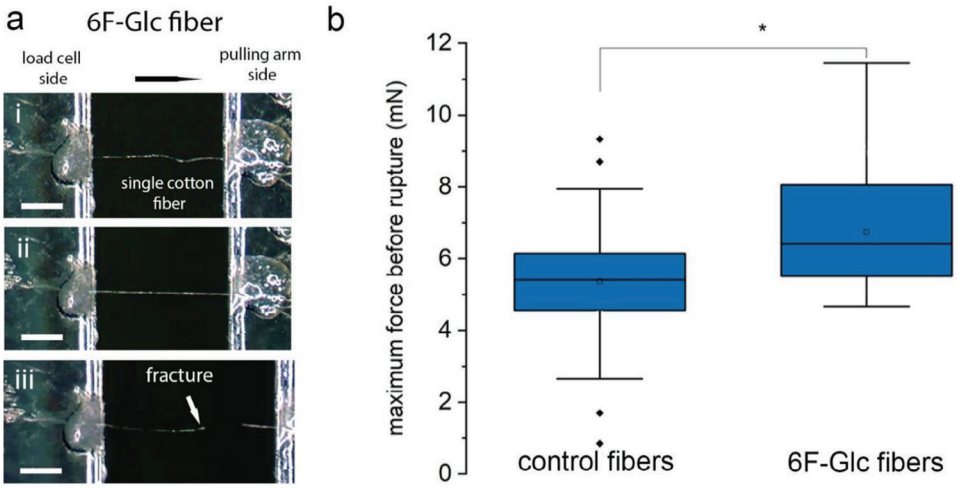

Figure 6. a) Representative sequence of images obtained during the tensile testing of single 6F-Glc fibers where i) represents the images showing the loosened fibers; ii) images showing the fibers at the maximum force/displacement before rupture; iii) images showing the fiber after failure, which is highlighted by the white arrow. Scale bar: 200 µm. The horizontal black arrow shows the direction of the movement of the holder end being pulled. b) Box plot of the maximum forces required for fracturing single cotton control and 6F-Glc fibers. The maximum forces were calculated by multiplying the load cell spring constant with the load cell deflection immediately before rupture. The mean maximum force for disrupting single cotton 6F-Glc fibers was statistically significant and 1.3-fold higher than the control fibers ($N = 38$ for each treatment, p-value < 0.05). The statistical analyses were performed by JASP software.[21]

2.4. Single Fiber Mechanical Properties

We used a homemade push-to-pull tensile tester to assess the mechanical properties of single cotton fibers (Figure S3). **Figure 6**a i–iii shows a sequence of images obtained during single 6F-Glc fibers cotton tensile testing from unstretched (Figure 6a–i) to rupture (Figure 6a–iii). We observed that when the fibers stretched, an unwinding of the convolutions occurred, which continued until they became completely deconvoluted before failing at maximum force. We determined the displacement (Δl) to be statistically significantly larger ($N = 38$ for each treatment, p-value < 0.05) for 6F-Glc fibers using Equation (3). Specifically, the 6F-Glc fibers show a mean displacement of 32.8 ± 9 µm, whereas the control fibers show a mean displacement of 27.6 ± 9 µm. In both cases, the large dispersion can be attributed to the natural variability of the cotton fibers. Subsequently, we calculated the maximum force required to disrupt single cotton fibers. We refrained from calculating stress-strain curves because of the large variability of cell wall thickness between fibers and within each fiber. Our analysis revealed a statistically significant difference in the mean maximum force required to disrupt single cotton fibers when comparing 6F-Glc and control fibers ($N = 38$ for each treatment, p-value < 0.05), that is, the mean maximum force for disrupting single cotton 6F-Glc fibers was 1.3-fold higher compared to the control fibers. Specifically, we calculated a mean maximum force of 5.3 ± 1.8 and 6.7 ± 1.6 mN for control and 6F-Glc fibers, respectively (Figure 6b) using Equation (4). The average values calculated for the displacement and maximum force before rupture are summarized in **Table 1**.

Table 1. Summary of the displacement (µm) and maximum force (mN) before rupture determined for 6F-Glc fibers and control fibers.

	Displacement [µm]	Maximum forces [mN]
Control fibers	27.6 ± 9	5.3 ± 1.8
6F-Glc fibers	32.8 ± 9	6.7 ± 1.6

3. Conclusion

In conclusion, this study demonstrates that the presence of glucose derivative 6F-Glc in the growth medium of in vitro cotton ovule cultures resulted in fluorine accumulation in the fibers and a remarkably low DS of 0.006, that is, for every 1000 AGU units, six hydroxyl groups were substituted. Our physical characterization shows that despite the low DS, the modification still has a significant impact on fiber structural and mechanical properties. The underlying mechanisms for these changes are not yet fully understood. Fluorine compounds, especially certain per- and poly-fluoroalkyl substances (PFAS), and their use in textiles have come under scrutiny in recent years due to environmental persistence and health concerns urging the research of alternative solutions. Future investigations will assess the biodegradability of 6F-Glc-based fibers in different environmental conditions. These studies, although still in vitro, will provide insights into fiber breakdown products and will contribute to a more comprehensive life-cycle assessment. Finally, this study highlights the potential of harnessing biological approaches in the development of future cellulose-based materials with novel or enhanced properties in a low DS regime.

4. Experimental Section

Cotton Plants and Fertilized In Vitro Ovule Culture Growth Conditions and Chemoenzymatic Synthesis of 6-Deoxy-6-fluoro-glucose (6F-Glc): Cotton (*G. hirsutum* L.) was grown in soil in a greenhouse between November 2021 and February 2022 at the Weizmann Institute of Science greenhouse facilities. Flowers were harvested at 2 dpa, and the ovary was

sterilized in a solution of NaOCl (6%) for 2 min at room temperature. The fertilized ovules were aseptically removed and placed floating onto sterile Beasley and Ting (BT) medium (15 mL) supplemented with gibberellic acid (GA, 5 µM), indoleacetic acid (IAA, 0.5 µM), and additives. The cultures were kept in the dark at 30 °C and under 5% CO_2 for 20 days (standard conditions).[22] 6-Deoxy-6-fluoro-glucose (6F-Glc) was synthesized by dissolving compound 2 (1.0 g; 2.86 mmol) in anhydrous MeOH (20 mL) and adding sodium methoxide solution (50 µL at 25%). The reaction was stirred at room temperature for 2 h, neutralized with resin (Dowex 50W X8), filtered, and concentrated under vacuum to afford 6F-Glc (3) (501 mg; 2.75 mmol; 96%). The first two steps of this route were performed as described in the previous work.[12] Then, 6F-Glc was added to the growth medium in two different concentrations (5 µM). After the end of the standard incubation, the cotton ovules were harvested. The fibers were carefully removed with the help of a sterile scalpel, washed five times with double distilled water, and maintained at −80 °C until further characterization.

Measurements of Ovule Length and Weight, and Fiber Length: Following the 20th day of growth under standard conditions, the control ovules and those incubated with 6F-Glc (5 µM) were washed extensively in double distilled water to remove any excess medium and were allowed to air-dry in a biological flow chamber. Measurements of ovule length and weight, and fiber length were carried out as described in a previous report.[23] Once dry, the ovules were weighed and placed in boiling distilled water for 2 min to relax the fibers. Next, each ovule was held under a running tap to straighten the fibers and dragged on filter paper to dry, and they were all aligned in the same direction. The aligned fibers were imaged using a Canon EDS M5 camera, and the ovule and fiber length were measured using ImageJ software. Once imaged, they were placed in an oven at 50 °C overnight to desiccate and weighed again the following day for dry matter content calculations. Next, the fiber bundle was carefully separated using a stainless steel scalpel and weighed separately. All statistical analysis was performed, and plots were created using JASP software (v 0.16.4).[21]

ToF-SIMS: ToF-SIMS measurements were performed using a TOF-SIMS NCS instrument, which combined a TOF.SIMS5 instrument (ION-TOF GmbH, Germany) and an in situ Scanning Probe Microscope (NanoScan, Switzerland) at Shared Equipment Authority from Rice University. Surface Spectrometry. Bunched 30 keV Bi_3^+ ions (with a measured current of 0.15 pA) were used as the primary probe for analysis (scanned area 500 × 500 µm^2) with a raster of 128 × 128 pixels. A charge compensation with an electron flood gun was applied during the analysis. The charge effects were adjusted using appropriate surface potential and adapted extraction bias depending on the analysis area and the polarity. The cycle time was fixed to 100 µs (corresponding to m/z = 0 – 911 a.m.u mass range). The primary ion dose density had been limited to 1.1012 ions per cm^2 to preserve the analyzed surface. For 2D imaging, bunched 60 keV Bi_3^+ ions (with a measured current of 0.05 pA) were used as the primary probe for imaging a field of view of 500 × 500 µm^2, with a raster of 2048 × 2048 pixels, and then the image raster was binned by a factor 64 to enhance the signal-to-noise ratio. A charge compensation with the electron flood gun was applied during the analysis. An adjustment of the charge effects was operated using a surface potential. The cycle time was fixed to 70 µs (corresponding to m/z = 0 – 446 a.m.u mass range). For depth profiling, bunched 30 keV Bi^{3+} ions (with a measured current of 0.15 pA) were used as the primary probe for depth profiling a field of view of 150 × 150 µm^2, with a raster of 64 × 64 pixels, and then the sputtering was performed using Ar_{1500}^+ ions at 10 keV with a typical current around 2.5 nA, and a rastered area of 500 × 500 µm^2. The beams were operated in non-interlaced mode, alternating one analysis cycle and one sputtering cycles (corresponding to 3.28 s) followed by a pause of 5 s for the charge compensation with an electron flood gun. Again, the charge effects had been adjusted using a surface potential. During the depth profiling, the cycle time was fixed to 200 µs (corresponding to m/z = 0 – 3645 a.m.u mass range). For data treatment, all data was treated and extracted using SurfaceLab 7.3. The ion signals from the spectra and from ion mappings were normalized using the total ion signal to standardize the values and to help for the comparison between the different samples or the area. A logarithmic color scale was used when the ion signal was too low to identify the local variations.

Scanning Electron Microscope (SEM), Elemental Analysis, and Degree of Substitution (DS): Washed fibers were excised from ovules fed with 6F-Glc (5 µM) and control were air-dried, glued onto a carbon stub, and imaged using a Phenom XL (ThermoFisher, Israel) using an acceleration voltage of 15 kV and vacuum of 1 Pa. 100 images were obtained from random positions with a magnification of 340x around carbon stub surface containing the fibers using a home-built python script. The fiber width was measured directly from SEM images using Fiji software (N = 25).[24] For elemental analysis, the elemental analysis dispersive X-ray (EDS) analysis built in the Phenom XL was used with an acceleration voltage of 15 kV and vacuum of 1 Pa and point as spot size. The data was collected in points on different 6F-Glc or control fibers (N = 10) or 2D maps. DS was calculated using Equation (1)[25] adapted to fluorine.

$$DS = (MGlc.wt\%F) / (100Mn - Mmat.wt\%F) \quad (1)$$

where DS is the degree of substitution, MGlc is the molar mass of the anhydroglucose unit (162 g mol^{-1}), Mn is the molar mass of the fluorine atom (19), Mmat is the molar mass of the fluorine introduced into the cellulose (19), and wt%F the fluorine content determined by elemental energy X-ray dispersive (EDS) analysis. All statistical analyses were performed using JASP software (v 0.16.4).[21]

Fourier Transform Infrared (FTIR) Spectroscopy: The samples were analyzed by FTIR spectroscopy. The samples were powdered and mixed with 5 mg of KBr. The mixture was pressed into a 7 mm disk using a PikeTM hand press and analyzed with a Thermo Nicolet iS5 FTIR spectrometer. FTIR spectra were collected by performing 32 scans with a resolution of 4 cm^{-1} wavenumbers. The FTIR spectra were collected using Omnic software. The measurements were performed at room temperature and in triplicate. The data were replotted and peak fitted using OriginLab Pro 2018 (b9.5.0193) using Gauss as peak function.

Wide-Angle X-Ray Scattering (WAXS): WAXS measurements were performed using a GANESHA instrument from SAXSLAB (Lyngby, Denmark) equipped with a Rigaku (Rigaku-Denki, Co., Tokyo, Japan) 40 W microfocused Cu source producing X-rays with a wavelength of λ = 1.54 Å detected by a Pilatus detector from Dectris (Baden, Switzerland). The 2D scattering data were radially and azimuthally averaged using standard reduction software (SAXSGUI, Lyngby, Denmark). The scattering patterns for the radially averaged intensity were recorded as a function of the scattering vector (Equation (2)).

$$q = 4\pi * \sin\theta / \lambda \quad (2)$$

where 2θ is the scattering angle and q was recorded in the range of 0.55 to 2.45 Å^{-1} in the WAXS configuration. The samples were mounted wet and gently aligned to form a fiber bundle and measured in vacuum. Measuring times were 900 s for WAXS. Radial averages were obtained from slices of 20 degrees angular opening parallel to the fiber axis. Cellulose WAXS patterns were calculated using the crystallographic data from ref.[20] using the Mercury package powder pattern calculator with FWHM set to 1 degree.[26]

Single Cotton Fiber Tensile Properties: The mechanical (tensile) tests of single cotton fibers were performed on our homemade push-to-pull tensile tester (Figure S3a, Supporting Information). The tester setup integrated a nanomanipulator (Kleindiek Nanotechnik, NanoControl NC-2-3. Germany), a load cell (Kleindiek Nanotechnik, STFMA SpringTable with the spring constant 106 N m^{-1}), and an arm that reversed the pushing force from the nanomanipulator to a pulling force that stretched the sample and deflected the load cell. Individual cotton fibers were carefully separated from a bundle with the help of an optical stereo microscope. The single fiber was then transferred onto a laser-cut polyester sample holder with a 1 mm diameter window, and both ends of the fiber were then fixed on the edge of the notch with epoxy glue and allowed to dry for 2 days at room temperature (Figure S3b, Supporting Information). The tests were monitored and recorded using a Carl Zeiss Stereomicroscope SteREO

Discovery.V12 at 23 °C and 45% relative humidity (RH). Movies were collected using an AMScope camera and respective acquisition software. It was ensured that both ends of the fiber were visible in the field of view throughout the whole test. The movies were split into single images. The displacement (Δl) was calculated by subtracting load cell deflection (Δx) from the deflection of the actuator (pulling arm) (a) using the formula (Equation (3)).

$$\Delta l = a - \Delta x \tag{3}$$

where Δl is the displacement, Δx is the load cell deflection, and (a) is the deflection of the actuator (pulling arm). The values for Δx and a were determined directly from the overlapping images in a loose fiber state and immediately before failure using Fiji/image J.[24] In the case of the force, Hooke's law was used (Equation (4)).

$$F = \mathrm{k} * \Delta x \tag{4}$$

where k and Δx are the spring constant (106 N m^{-1}) and the deflection of the load cell, respectively, assuming the stiffness of the setup is much higher than that of the cotton fiber. The movement of the fiber end close to the load cell was followed and used as the deflection of the load cell. For each type of fiber, seven specimens were measured for statistical reasons. All statistical analyses (descriptive) were performed using JASP software (v 0.16.4).[21]

Supporting Information

Supporting Information is available from the Wiley Online Library or from the author.

Acknowledgements

O.A.K. and P.A. contributed equally to this work. The authors want to thank Dr. XiaoMeng Sui (Weizmann Institute of Science, Israel) for the helpful discussions on single fiber tensile testing. This work was financially supported by the European Union, ERC Consolidator project" BIOMATFAB" (Project #101045466), GIF German-Israeli Foundation for Scientific Research and Development research grant (Project #I-1509-302.5/2019), MINERVA Stiftung (Project # 136809), with funds from the BMBF of the Federal Republic of Germany, Benoziyo Endowment Fund for the Advancement of Science, Estate of Raymond Lapon and Estate of Olga Klein Astrachan; the Yeda-Sela Center for Basic Research; the Abramson Family Center for Young Scientists (Weizmann Institute of Science, Rehovot, Israel); and the University of Manchester. ToF-SIMS analyses were carried out with support provided by the Shared Equipment Authority at Rice University. Views and opinions expressed are, however, those of the only and do not necessarily reflect those of the European Union or the European Research Council. Neither the European Union nor the granting authority can be held responsible for them.

Conflict of Interest

The authors declare no conflict of interest.

Data Availability Statement

The data that support the findings of this study are openly available in GitHub at https://github.com/fnatalio/6FGlc_cotton, reference number 1234.

Keywords

cellulose, mechanical properties, modification cellulose, structures

Received: September 22, 2023
Revised: November 3, 2023
Published online: December 10, 2023

[1] a) K. N. Onwukamike, S. Grelier, E. Grau, H. Cramail, M. A. R. Meier, *ACS Sustainable Chem. Eng.* **2019**, *7*, 1826; b) X. Zhou, X. Lin, K. L. White, S. Lin, H. Wu, S. Cao, L. Huang, L. Chen, *Cellulose* **2016**, *23*, 811; c) K. Petzold, A. Koschella, D. Klemm, B. Heublein, *Cellulose* **2003**, *10*, 251; d) D. Klemm, A. Stein, *J. Macromol. Sci., Part A: Pure Appl.Chem.* **1995**, *32*, 899; e) T. Heinze, K. Schwikal, S. Barthel, *Macromol. Biosci.* **2005**, *5*, 520; f) D. Klemm, B. Philpp, T. Heinze, U. Hewinze, W. Wagenknecht, *Comprehensive Cellulose Chemistry: Functionalization of Cellulose*, Vol. 2, Wiley-VCH, **1998**; g) T. Heinze, T. Liebert, *Prog. Polym. Sci.* **2001**, *26*, 1689; h) D. Klemm, T. Heinze, B. Philipp, W. Wagenknecht, *Acta Polym.* **1997**, *48*, 277; i) B. Ly, W. Thielemans, A. Dufresne, D. Chaussy, M. N. Belgacem, *Compos. Sci. Technol.* **2008**, *68*, 3193; j) P. Trivedi, P. Fardim, in *Production of Materials from Sustainable Biomass Resources* (Eds: Z. Fang, R. L. Smith, Jr, X.-F. Tian), Springer, Singapore **2019**, p. *99*.
[2] a) R. R. M. De Freitas, A. M. Senna, V. R. Botaro, *Ind. Crops Prod.* **2017**, *109*, 452; b) A. Casaburi, Ú. Montoya Rojo, P. Cerrutti, A. Vázquez, M. L. Foresti, *Food Hydrocolloids* **2018**, *75*, 147.
[3] T. Heinze, *Cellulose Chemistry and Properties: Fibers, Nanocelluloses and Advanced Materials. Advances in Polymer Science* (Eds: O. Rojas) Springer, Cham **2015**, *271* https://doi.org/10.1007/12_2015_319
[4] a) M. Schnabelrauch, S. Vogt, D. Klemm, I. Nehls, B. Philipp, *Angew. Makromol. Chem.* **1992**, *198*, 155; b) T. Liebert, M. Schnabelrauch, D. Klemm, U. Erler, *Cellulose* **1994**, *1*, 249; c) T. Liebert, D. Klemm, *Acta Polym.* **1998**, *49*, 124; d) K. Zhang, D. Peschel, E. Bäucker, T. Groth, S. Fischer, *Carbohydr. Polym.* **2011**, *83*, 1659.
[5] T. Heinze, S. Hornig, Versatile concept for the structure design of polysaccharide-based nanoparticles **2010**. https://pubs.acs.org/doi/10.1021/bk-2009-1017.ch009
[6] W. G. Glasser, B. K. Mccartney, G. Samaranayake, *Biotechnol. Prog.* **1994**, *10*, 214.
[7] D. S. Bao, C. F. Liu, R. C. Sun, *Adv. Mater. Res.* **2012**, *554*, 244.
[8] W. Y. Li, A. X. Jin, C. F. Liu, R. C. Sun, A. P. Zhang, J. F. Kennedy, *Carbohydr. Polym.* **2009**, *78*, 389.
[9] M. Han, X. Wu, Y. Peng, H. Yu, *J. Food Process. Preserv.* **2022**, *46*, 16125.
[10] V. Espinosa-Solis, Y. V. García-Tejeda, E. J. Leal-Castañeda, V. Barrera-Figueroa, *Polymers* **2020**, *12*, 2548.
[11] G. S. Bulmer, P. De Andrade, R. A. Field, J. M. Van Munster, *Carbohydr. Res.* **2021**, *508*, 108411.
[12] P. De Andrade, J. C. Muñoz-García, G. Pergolizzi, V. Gabrielli, S. A. Nepogodiev, D. Iuga, L. Fábián, R. Nigmatullin, M. A. Johns, R. Harniman, S. J. Eichhorn, J. Angulo, Y. Z. Khimyak, R. A. Field, *Chemistry* **2021**, *27*, 1374.
[13] R. Nigmatullin, P. De Andrade, R. Harniman, R. A. Field, S. J. Eichhorn, *Langmuir* **2021**, *37*, 9215.
[14] F. Natalio, R. Fuchs, S. R. Cohen, G. Leitus, G. Fritz-Popovski, O. Paris, M. Kappl, H.-J. Butt, *Science* **2017**, *357*, 1118.
[15] T. Rodríguez-Pérez, I. Lavandera, S. Fernández, Y. S. Sanghvi, M. Ferrero, V. Gotor, *Eur. J. Org. Chem.* **2007**, *2007*, 2769.
[16] S. G. Withers, M. D. Percival, I. P. Street, *Carbohydr. Res.* **1989**, *187*, 43.
[17] F. Natalio, *Isr. J. Chem.* **2020**, *60*, 1197.
[18] F. Natalio, R. Maria, *Fibers* **2018**, *6*, 11.
[19] a) S. Y. Oh, D. I. Yoo, Y. Shin, G. Seo, *Carbohydr. Res.* **2005**, *340*, 417; b) S. Y. Oh, D. I. Yoo, Y. Shin, H. C. Kim, H. Y. Kim, Y. S. Chung, W. H. Park, J. H. Youk, *Carbohydr. Res.* **2005**, *340*, 2376.
[20] A. D. French, *Cellulose* **2014**, *21*, 885.
[21] J. Love, R. Selker, M. Marsman, T. Jamil, D. Dropmann, J. Verhagen, A. Ly, Q. F. Gronau, M. Smíra, S. Epskamp, D. Matzke, A. Wild, P. Knight,

J. N. Rouder, R. D. Morey, E.-J. Wagenmakers, *J. Stat. Software* **2019**, *88*, 1.

[22] a) C. A. Beasley, *Science* **1973**, *179*, 1003; b) C. A. Beasley, I. P. Ting, *Am. J. Bot.* **1974**, *61*, 188.

[23] X. Li, W. Liu, Z. Ren, X. Wang, J. Liu, Z. Yang, J. Zhao, X. Pei, Y. Liu, K. He, F. Zhang, Z. Zhang, D. Yang, X. Ma, W. Li, *J. Exp. Bot.* **2022**, *73*, 711.

[24] J. Schindelin, I. Arganda-Carreras, E. Frise, V. Kaynig, M. Longair, T. Pietzsch, S. Preibisch, C. Rueden, S. Saalfeld, B. Schmid, J.-Y. Tinevez, D. J. White, V. Hartenstein, K. Eliceiri, P. Tomancak, A. Cardona, *Nat. Methods* **2012**, *9*, 676.

[25] a) V. P. Robson, E. G. Thais, A. P-d-S. Marcelo, S. F. Kênia, J. d. M. Aparecido, in *Nanofibers* (Ed.: K. Brajesh), IntechOpen, Rijeka, Croatia **2021**, Ch. 7; b) C. Vaca-Garcia, M. E. Borredon, A. Gaseta, *Cellulose* **2001**, *8*, 225.

[26] C. F. Macrae, I. Sovago, S. J. Cottrell, P. T. A. Galek, P. Mccabe, E. Pidcock, M. Platings, G. P. Shields, J. S. Stevens, M. Towler, P. A. Wood, *J. Appl. Crystallogr.* **2020**, *53*, 226.

